# Estimation of Design Parameters of Single-Phase Distribution Transformers From Terminal Measurements

Reza Kazemi, *Student Member, IEEE*, Saeed Jazebi, *Senior Member, IEEE*, Digvijay Deswal, *Student Member, IEEE*, and Francisco de León, *Fellow, IEEE*

***Abstract*—In this paper, a novel method is proposed for the estimation of the design parameters of single-phase distribution transformers using data acquired from terminal measurements along with nameplate data and external tank dimensions. Transformer parameters that can be measured from terminals, for example, leakage inductance, saturation inductance, and winding resistance, are considered first. These parameters are analytically correlated with the geometrical information of the transformer structure. A system of nonlinear equations is derived accordingly. Winding dimensions and the number of turns are computed with acceptable engineering accuracy. The core dimensions (including its cross-sectional area) are calculated using winding information. The obtained data can be utilized to develop white- or gray-box models to be used in the investigation of the thermal and/or electromagnetic behavior of power transformers as presented in several research studies published to date. Examples on laboratory and utility-grade transformers are shown for illustration and validation of the proposed design parameter estimation method.**

***Index Terms*—Leakage inductance, parameter estimation, saturation inductance, transformer design.**

## I. Introduction

DERIVATION of physically realizable models to represent the internal electromagnetic or thermal behavior of power transformers presents an important challenge. Researchers have developed transformer models using terminal measurements and assumptions on common design practice in the past [1]–[3]. Accurate models capable of representing the transformer behavior under wide working conditions require the knowledge of the design parameters [4]–[7]. The detail design data is usually unavailable for old equipment or inaccessible due to intellectual property rights of the manufacturing companies. Measurement of the parameters by opening the transformer is destructive, expensive, and not feasible for industrial consumers, utilities or other end users in most cases. Alternatively, the design parameters such as dimensions of the windings, number of turns in each winding, and dimensions of the core structure (yokes and limbs), can be estimated using nameplate data and information obtained from terminal measurements. This method is practical both in field and laboratory settings.

There are very few research studies published on the estimation of transformer design parameters. In [8], the authors have utilized the nameplate information and common design practices combined with external dimensions of the tank to obtain an initial approximation of the range of some of the transformer design parameters. The proposed method is straightforward. However, it is not capable of calculating crucial parameters such as thickness and height of windings, the radii of the internal windings or inter-winding insulation spaces.

In this paper, transformer characteristics such as winding resistances, leakage inductance, and saturation inductances are obtained from terminal measurements. Since the aforementioned characteristics are functions of the transformer design parameters, design formulae and measured values can be used to write a set of equations. This system of equations is solved using a non-linear least-square method to estimate the radius, height, and thickness of all windings, in addition to the number of turns in each winding. The estimated winding information is then utilized to calculate the transformer core geometrical information including the cross sectional area and the length of the limbs and yokes.

The proposed method is successfully applied to the identification of the construction dimensions of five single-phase transformers of various sizes (from 1 to 167 kVA). The obtained results show good precision when compared with the actual design values. The presented method can be applied to a wide range of single-phase three-limb distribution transformers with concentric windings. In practice, however, such transformers usually exist in the range of up to 167 kVA. Since the analytical expressions are general, the method is applicable to either disk or layer windings. The arrangement of the separate turns and number of winding layers has limited impact on the accuracy of the proposed method because of the low frequency nature of the measurement tests used to formulate the problem. In addition the method is based on the inner dimensions of the transformer rather than the external tank dimensions, or assumptions made on the manufacturing practices that vary widely with the transformer capacity and the utilized accessories, such as tap changers, relays, etc. This produces a method potentially applicable to a wide range of transformer sizes.

Manuscript received March 7, 2016; revised June 2, 2016, August 2, 2016, and September 22, 2016; accepted October 24, 2016. Date of publication October 26, 2016; date of current version May 19, 2017. Paper no. TPWRD-00283-2016.

The authors are with the Department of Electrical and Computer Engineering, New York University, Brooklyn, NY 11201 USA (e-mail: kazemi@nyu.edu; jazebi@ieee.org; dd1681@nyu.edu; fdeleon@nyu.edu).

Color versions of one or more of the figures in this paper are available online at http://ieeexplore.ieee.org.

Digital Object Identifier 10.1109/TPWRD.2016.2621753

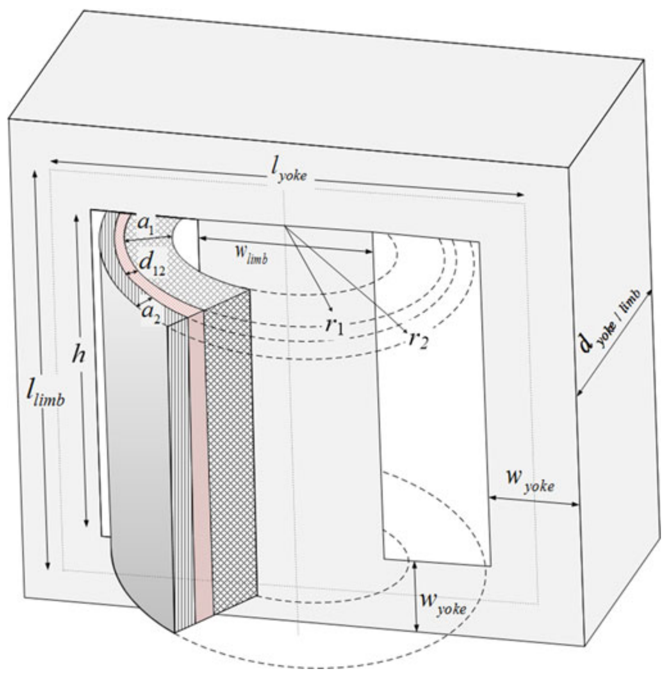


Fig. 1. Core and winding configurations of a single-phase three-limb transformer.

The obtained data can be used for constructing white-box models for the study of low frequency phenomena, such as inrush currents, ferroresonance and geomagnetically induced currents [10]. It can also be utilized to derive parameters of the ladder-type gray-box models that represent the transformer internal behavior up to 1 MHz [11], [12]. These models are popular to detect axial and radial deformations and displacements of the windings that are consequences of mechanical stresses produced by short circuit currents or transportation. This can be done with the comparison of FRA plots before and after an incident [13], [14]. The obtained design parameters are also necessary to derive steady state or transient thermal models where internal dimensions are required [15].

## II. Problem Formulation

For the estimation of winding information, it is necessary to measure the transformer electrical characteristics. Analytical formulae for the same characteristics as functions of transformer internal dimensions and material properties are utilized to correlate the measured values with the geometrical information of the windings. To avoid unnecessary complications, the windings are assumed to be cylindrical.

The geometrical configuration of a single-phase two-winding three-limb power transformer is depicted in Fig. 1. This figure introduces the parameters that are to be estimated: $a_1$ and $r_1$ represent the thickness and mean radius of the inner-most winding. Similarly, $a_2$ and $r_2$ are mean thickness and radius of the outer-most winding, $h$ is the average height of the windings and $d_{12}$ is the inter-winding distance. $l_{yoke}$ is the length of the yoke and $l_{limb}$ is the length of the limb.

The cross section of the limb is assumed to be square for small transformers for simplicity, meaning the width ($w_{limb}$) and depth ($d_{limb}$) of the limb are considered to be the same. The cross section of the yoke is assumed to have a rectangular shape. The yoke cross sectional area is taken as half of the limb cross sectional area as each yoke carries half of the flux (since optimally they are designed at the same flux density). For large transformers, the core cross section is circular similar to the windings. In this case, $w_{limb}$ and $w_{yoke}$ would become equal to the diameter and radius of the limb respectively. This is further discussed in Section IV.

In the next sections, an example of a single-phase 4-winding transformer has been presented to illustrate the measurement setups and discuss the utilized formulae.

### A. Leakage Inductance

The leakage inductance between each pair of windings is measured using standard short circuit tests [16]. The measurements are carried out taking two windings at a time, energizing one, while another is short-circuited, and all other windings are in open circuit [17]. For example, the leakage inductance between windings 1 and 2 ($L_{12}$) is measured from winding 1 while winding 2 is in short circuit and the other two windings (3 and 4) are in open circuit

The distribution of the leakage flux across the windings depends on the dimensions and geometrical configuration of the windings. A simple schematic of the geometrical arrangement of the windings is depicted in Fig. 2(a). A trapezoidal flux distribution is assumed for the leakage flux between each pair of windings [18]. For each case the flux increases linearly across the inner winding thickness, remains constant in the inter-winding space (insulation), and decreases linearly along the outer winding thickness; see Fig. 2(b). The leakage inductance for each pair of the windings can be calculated as follows [18]:

$$L_{ij} = \frac{\mu_0 N^2 l_{ij}}{h}\left[\frac{a_i}{3} + d_{ij} + \frac{a_j}{3}\right] \quad (1)$$

where *N* is the common number of turns, $l_{ij}$ is the mean length of the winding turns, $h$ is the average effective height of the windings (all windings are assumed to have the same height for simplicity), $a_i$ is the mean thickness of winding *i* and $d_{ij}$ is the distance between winding *i* and *j*.

Assuming cylindrical geometry for the windings $l$ can be expressed as:

$$l_{ij} = \pi(r_i + r_j) \quad (2)$$

where $r_i$ is the mean radius of winding *i*.

Although the flux was assumed to have a linear distribution, fringing effects often cannot be neglected especially for the non-adjacent windings in a multi-winding transformer. To take fringing effect in to account, the winding effective height is calculated using the Rogowski factor [19]. The Rogowski factor is a function of the windings and the inter-winding insulating thicknesses and can be calculated as follows:

$$K_R = 1 - \frac{(a_i + a_j + d_{ij})(1 - e^{-\pi h/(a_i + a_j + d_{ij})})}{\pi h} \quad (3)$$

Hence, the final relation for the leakage inductance is given by:

$$L_{ij} = \frac{\mu_0 N^2 \pi\,(r_i + r_j)}{K_R\, h}\left[\frac{a_i}{3} + d_{ij} + \frac{a_j}{3}\right] \quad (4)$$

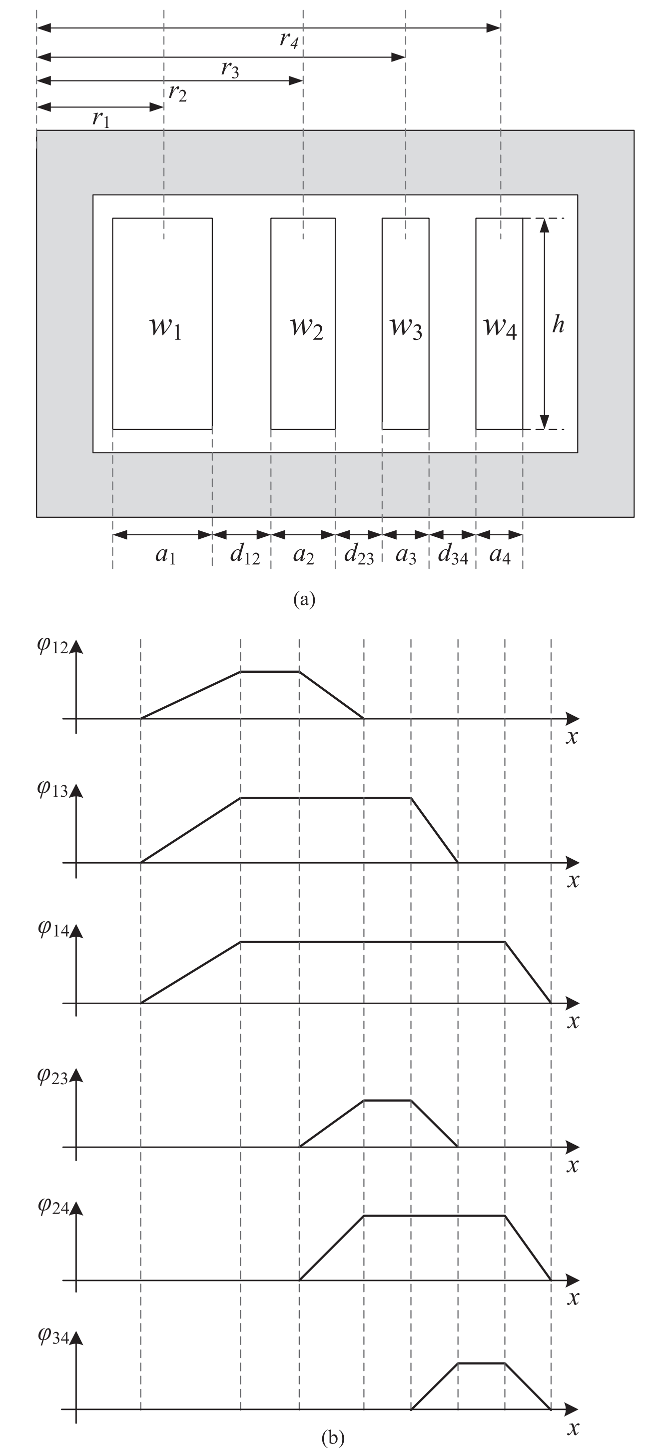


Fig. 2. (a) Geometrical configuration of the windings and core shown on the right half side of the transformer frame (single-phase three-limb core); (b) trapezoidal flux distribution along the windings and in the inter-winding insulator spaces.

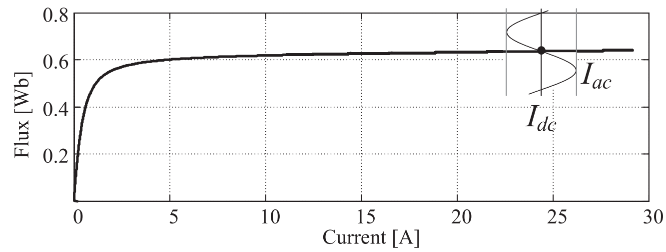


Fig. 3. Positive part of the saturation curve and operation of transformer with a dc-biased ac excitation around a deep saturation operation point [20].

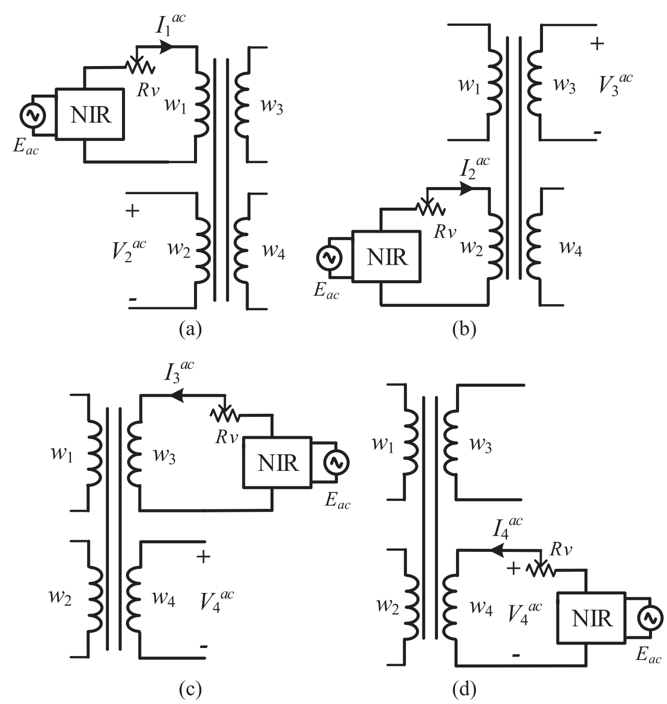


Fig. 4. Test setups to measure saturation inductance of each winding in a 4-winding transformer using a non-ideal rectifier (NIR); (a) $L^1_{sat}$, (b) $L^2_{sat}$, (c) $L^3_{sat}$, (d) $L^4_{sat}$.

## B. Saturation Inductance

To measure the saturation inductance, a hybrid (dc-biased ac) source is used to drive the transformer core in to deep saturation [20]. In saturation the ac component sweeps on the linear (saturated) region of the magnetizing characteristic around the dc operating point; see Fig. 3. A non-ideal rectifier with natural ac voltage ripple has been utilized as the voltage source as shown in the test setup of Fig. 4. The voltage measurement is taken from the secondary winding to eliminate the effect of the voltage drop caused by the resistance of the excited winding. The selection of the secondary winding can have an effect on the measurement results. To improve the measurement accuracy, it is recommended to measure the voltage on the adjacent outer winding of the winding being excited rather than inner or outer windings, so that almost all the flux coming out of the excited winding can be captured. As illustrated in Fig. 5 taking the measurement on the inner or outer windings can introduce measurement errors since not all flux would be captured. For measuring the saturation inductance of the outer-most winding the voltage needs to be measured on the same winding. Thus the voltage drop on the winding resistance needs to be considered. This latter method can be applied similarly to any of the other windings when the position of the windings is not known. In our experience, caution must be used when subtracting the resistive voltage drop. Winding resistance changes with

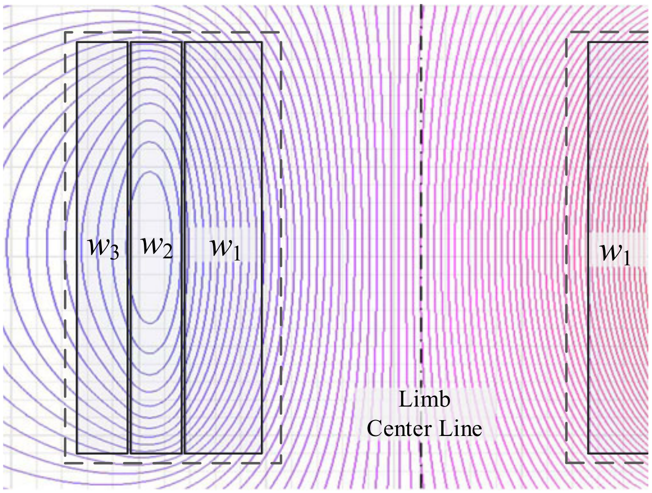


Fig. 5. Illustration of magnetic flux lines of transformer windings in saturation inductance test with the middle winding ($w_2$) excited.

temperature and frequency during the test. For better accuracy, the resistance should be measured right after the test or extracted from the voltage and current wave shapes using FFT. There are also alternate methods to measure transformer deep saturation characteristics with low power sources; see references [21]–[24] for example.

Based on the harmonic frequency content of the utilized non-ideal rectifier, the fundamental component or any dominant triplen harmonic of the measured voltage and current can be extracted from the recorded signals. Fast Fourier Transform (FFT) is utilized for this purpose and results are used to calculate the saturation inductance as below [20]:

$$L_{sat} = \frac{V^h}{2\pi f n I^h} \tag{5}$$

where $V^h$ and $I^h$ are the amplitude of fundamental or harmonic components of the measured voltage and current as shown in Fig. 4, $f$ is the harmonic component frequency, and $n$ is the turns ratio. Although all the harmonic components are supposed to return very similar numbers, to guarantee best results it is recommended to use the dominant rectifier harmonic for the calculations.

The saturation inductance can be calculated directly using the geometrical dimensions of the windings. Increasing the winding excitation up to the core deep saturation region causes the permeability of the iron to reduce steeply as the flux density increases until it reaches the permeability of air. In this situation, it can be assumed that the incremental flux closes its path solely through the air. A closed form expression to calculate the inductance of coaxial concentric single-layer coils is presented in [25]. In [26] the authors applied Barky's transformation to the elliptical integrals that had simplified and reduced the air-core inductance expressions. The saturation inductance can be calculated using the following expression [26]:

$$L^i_{sat} = 4\pi\mu_0 \left(\frac{N}{h}\right)^2 r_i^3 \left(M_i(r_i, h) - \frac{2\pi}{3}\right) \tag{6}$$

where:

$$M_i(r_i, h) = \frac{2}{\pi} \int_0^{\frac{\pi}{2}} \frac{\sin^2\varphi}{3\sqrt{{k_i}^2 \cos^2\varphi + \sin^2\varphi}}\, d\varphi \tag{7}$$

$$k_i = \sqrt{\frac{h^2}{4{r_i}^2 + h^2}} \tag{8}$$

and $\varphi$ is the azimuthal angle. The expression returns accurate values for the windings when the radius assumed to be much larger than the winding thickness which is a valid assumption for transformer windings.

### C. DC Resistance

The very small dc resistance of a winding can be measured with a Kelvin Bridge. Simultaneously, the dc resistance depends on the geometry, wire gauge, and the number of turns of the winding. An expression for the calculation of the dc resistance can be obtained by expanding the basic resistance formula as follows:

$$R^i_{dc} = \frac{\rho L}{A} = \frac{\rho(2\pi r_i N)}{\left(\frac{ff\, h\, a_i}{N}\right)} = \frac{2\pi\rho r_i N^2}{ff\, h\, a_i} \tag{9}$$

where $\rho$ is the resistivity of the conductor, *ff* is the filling factor of the winding, $A$ is the winding cross sectional area, $L$ is the total length of the winding conductor and all other parameters are the same as defined for (1). Parameter *ff* gives a measure of the density of the conductors in the cross sectional area of the winding. Note that, *ff* is also obtained in the estimation process along with the other physical characteristics of the transformer.

### D. Geometrical Relations

Simple geometry can be used to derive additional equations for the problem formulation. As illustrated in Fig. 2(a), the radius of any winding can be calculated using the dimensions of the adjacent windings and insulation thicknesses. The radius of any winding (except the inner-most) can be calculated by adding the radius of the adjacent inner winding to the insulation thickness in between the windings and half of the thickness of each winding as:

$$r_{i+1} = r_i + \frac{a_i}{2} + d_{i,i+1} + \frac{a_{i+1}}{2} \tag{10}$$

For instance, the radius of winding 2, ($r_2$) can be calculated using the dimensions of the adjacent inner winding ($r_1$ and $a_1$) together with the insulation thickness in between the windings ($d_{12}$) as follows:

$$r_2 = r_1 + \frac{a_1}{2} + d_{12} + \frac{a_2}{2}$$

### E. Completing the System of Equations

When the number of unknown design parameters exceeds the number of equations that could be derived using the transformer characteristics, additional equations are needed to be used. In particular, the number of turns in any winding can also be calculated directly as a function of transformer parameters according to Faraday's law. The number of turns for any winding has a relation with the induced voltage in the winding as [18]:

$$V = 4.44 f N A_{\mathit{eff}} B_{\max} = 4.44 f \cdot N \cdot SF \cdot A \cdot B_{\max} \quad (11)$$

In this relation, $f$ is the nominal frequency, $A_{\mathit{eff}}$ and $A$ are the effective and physical core limb cross-sectional area respectively, *SF* is the core stacking factor that can range from 0.9 to 0.98 for power transformers [31] and $B_{\max}$ is the maximum design flux density. Depending on the transformer size and rating, the maximum flux density can have a value between 1.5 T (for small transformers) and 1.8 T (for large transformers). The nominal voltage and frequency are also known through nameplate data and the core limb cross sectional area can be replaced by the relation that calculates $A$ (the mechanical cross section) using the innermost winding information as shown in Section IV. Consequently, the number of turns can be estimated from:

$$N = \frac{V}{4.44 f A_{\mathit{eff}} B_{\max}} = \frac{V}{4.44 f \cdot SF \cdot A \cdot B_{\max}} \quad (12)$$

For dual voltage transformers (e.g. secondary at 120–240 V), the windings are similar and additional equations can be used to give better results. For instance, the winding thicknesses and insulation system is assumed to be the same, which reduces the number of unknowns and guarantees consistency of winding dimensions.

### F. System of Equations

Equations (1)–(12) along with the terminal measurements are used to construct a set of non-linear equations as follows:

$$\begin{cases} f_k = L_{ij}^{mes} - L_{ij}^{cal(n)}(N, h, r_i, r_j, a_i, a_j, d_{ij}) = 0 \\ f_l = L^{i\,mes}_{sat} - L^{i\,cal(n)}_{sat}(N, h, r_i) = 0 \\ f_o = R^{i\,mes}_{dc} - R^{i\,cal(n)}_{dc}(N, h, r_i, a_i, ff) = 0 \\ f_p = r_i^{cal(n-1)} - r_i^{cal(n)}(r_{i-1}, a_{i-1}, a_i, d_{i,i-1}) = 0 \\ \qquad\qquad\qquad\qquad\qquad\qquad i \geq 2 \\ f_q = N^{cal(n-1)} - N^{cal(n)}(r_1, a_1, d_{12}) = 0 \end{cases} \quad (13)$$

The superscripts *mes* and *cal* indicate the measured and calculated values respectively and the superscript (*n*) represents the value of the variable at the *n*th iteration. Subscript $k$ is within $1 \leq k \leq m(m-1)/2$ where $m$ is the number of the windings of the transformer. Subscript $l$ is within $k_{\max} < l \leq k_{\max} + m$. Subscript $o$ is within $l_{\max} < o \leq l_{\max} + m$. Similarly, Subscript $p$ is within $o_{\max} < p \leq o_{\max} + m - 1$ and finally $q = p_{\max} + 1$. In total, minimum of $m(m+5)/2$ equations can be derived for our estimation problem. The obtained non-linear set of equations is solved numerically to obtain the intended winding design parameters.

## III. Numerical Results of the Estimation of Winding Parameters

To solve the set of equations given in (13), a bounded, non-linear, least-square method is used to minimize the error. To guarantee the best results and shortest computing time, the problem has been bounded with constraints based on the outer dimensions of the transformer, common design practices, and nameplate information. The height of the tank is used to bound the height of the windings and the width of the tank is utilized to bound the outermost winding radius. The BIL values (available on the nameplate or known from the test sheet) are used to bound the insulation thicknesses. The boundaries for winding thicknesses were set according to assumptions on common design practice on voltage per turn and current densities of the wires [27]. The number of turns can be bounded using the same information as for winding thicknesses. With the boundaries for winding thicknesses and the outermost winding, the boundaries for the inner windings can be set respectively [8], [27].

The utilized method minimizes the second norm of the obtained expressions which are functions of transformer winding parameters. The equations consist of the difference between the values obtained by measurements and calculated with the proposed formulae or the difference between values calculated through formulae in current and previous iterations expressed as:

$$\min\left(\|F(r_1, r_2, ..., r_i, a_1, a_2, ..., a_i, d_{12}, d_{23}, ..., d_{ij}, h, N)\|\right) = \min \begin{pmatrix} {f_1}^2(r_1, r_2, ..., r_i, a_1, a_2, ..., a_i, d_{12}, d_{23}, ..., d_{ij}, h, N) \\ {f_2}^2(r_1, r_2, ..., r_i, a_1, a_2, ..., a_i, d_{12}, d_{23}, ..., d_{ij}, h, N) \\ ... \\ {f_n}^2(r_1, r_2, ..., r_i, a_1, a_2, ..., a_i, d_{12}, d_{23}, ..., d_{ij}, h, N) \end{pmatrix} \quad (14)$$

The solution of this system of equations gives the design parameters of the windings. The proposed method has been applied to five single-phase transformers with different ratings (1, 1.8, 5, 75, and 167 kVA) and characteristics to validate the accuracy and the range of applicability.

The estimation results for winding parameters of a 4-winding, 1 kVA, 120–240/120–240 V, single-phase transformer are presented in Table I. Since the transformation ratio is one, all windings have the same number of turns (*N*). The errors are small for all of the parameters (10% in worst case). The results for a 4-winding, 1.8 kVA, 120–240/120–240 V, single-phase

TABLE I
Estimated Winding Parameters of a 4-Winding, 1 kVA, 120–240/120–240 V, Single-Phase Transformer

| Parameter | Actual | Estimated | Error (%) |
|---|---|---|---|
| $r_1$ | 38.1 mm | 40.3 mm | 5.8 |
| $r_2$ | 44.3 mm | 45.8 mm | 3.5 |
| $r_3$ | 50.4 mm | 51.6 mm | 2.3 |
| $r_4$ | 56.4 mm | 57.2 mm | 1.5 |
| $a_1$ | 4.85 mm | 4.79 mm | –1.2 |
| $a_2$ | 4.85 mm | 5.19 mm | 7.1 |
| $a_3$ | 4.85 mm | 5.17 mm | 6.6 |
| $a_4$ | 4.85 mm | 5.05 mm | 4.1 |
| $d_{12}$ | 0.5 mm | 0.55 mm | 10.1 |
| $d_{23}$ | 0.5 mm | 0.54 mm | 9.5 |
| $d_{34}$ | 0.5 mm | 0.54 mm | 9.6 |
| $h$ | 63 mm | 63.5 mm | 0.8 |
| $N$ | 108 | 105 | –2.8 |

TABLE II
ESTIMATED WINDING PARAMETERS OF A 4-WINDING, 1.8 kVA, 120–240/120–240 V, SINGLE-PHASE TRANSFORMER

| Parameter | Actual | Estimated | Error (%) |
|---|---|---|---|
| $r_1$ | 47 mm | 46.6 mm | –0.7 |
| $r_2$ | 50 mm | 50.4 mm | 0.9 |
| $r_3$ | 52 mm | 54.1 mm | 4.1 |
| $r_4$ | 55 mm | 57.7 mm | 4.9 |
| $a_1$ | 3.8 mm | 3.58 mm | –5.8 |
| $a_2$ | 3.8 mm | 3.58 mm | –5.8 |
| $a_3$ | 3.8 mm | 3.33 mm | –12.3 |
| $a_4$ | 3.8 mm | 3.46 mm | –8.5 |
| $d_{12}$ | 0.22 mm | 0.20 mm | –8.1 |
| $d_{23}$ | 0.22 mm | 0.20 mm | –9.1 |
| $d_{34}$ | 0.22 mm | 0.20 mm | –9.1 |
| $h$ | 70.0 mm | 71.4 mm | 2.0 |
| $N$ | 132 | 146 | 10.6 |

TABLE III
ESTIMATED WINDING PARAMETERS OF A 4-WINDING, 5 kVA, 120–240/480–960 V, SINGLE-PHASE TRANSFORMER

| Parameter | Actual | Estimated | Error (%) |
|---|---|---|---|
| $r_1$ | 67.1 mm | 68.9 mm | 2.8 |
| $r_2$ | 71.9 mm | 72.6 mm | 1.0 |
| $r_3$ | 80.6 mm | 77.8 mm | –3.4 |
| $r_4$ | 86.7 mm | 84.2 mm | –2.8 |
| $a_1$ | 3.1 mm | 3.37 mm | 8.9 |
| $a_2$ | 3.1 mm | 2.84 mm | –8.2 |
| $a_3$ | 5.5 mm | 5.75 mm | 4.6 |
| $a_4$ | 5.5 mm | 5.8 mm | 5.4 |
| $d_{12}$ | 0.56 mm | 0.59 mm | 7.3 |
| $d_{23}$ | 0.84 mm | 0.9 mm | 7.4 |
| $d_{34}$ | 0.56 mm | 0.59 mm | 7.3 |
| $h$ | 85.7 mm | 86.7 mm | 3.5 |
| $N$ | 30 | 30 | 0 |

transformer are given in Table II. The results for this case also show good accuracy for all parameters (around 12% in the worst case). For the 5 kVA, 120–240/280–960 V single-phase transformer, results are presented in Table III. The estimation errors for all design parameters are again small (under 9% in the worst case).

For further validation of the method two utility-grade transformers, one rated at 75 kVA, 7.2 kV/120–240 V and another one rated at 167 kVA, 14.4 kV/120–240 V were used. Detailed construction information along with standard test data were utilized to build a 3D finite element model of the transformer. All the measurement tests described in Section II have been carried out using finite element simulations to obtain the required transformer characteristics. The proposed estimation method has been applied to obtain the design parameters subsequently. The results, presented in Tables IV and V, show that the largest error is 8% for the 75 kVA transformer and under 7% for the 167 kVA transformer. Overall, the results from the five cases show acceptable engineering accuracy.

Note that not all errors come from the accuracy of the method itself. There are always some discrepancies between the design values and the final product. Some of the dimensions, such as winding thicknesses or radii, are not uniform along the

TABLE IV
ESTIMATED WINDING PARAMETERS OF A UTILITY 75 kVA, 7.2 kV–120/240 V, SINGLE-PHASE TRANSFORMER

| Parameter | Actual | Estimated | Error (%) |
|---|---|---|---|
| $r_1$ | 101.4 mm | 102.7 mm | 1.2 |
| $r_2$ | 130.3 mm | 132.7 mm | 1.9 |
| $r_3$ | 159.2 mm | 162.8 mm | 2.3 |
| $a_1$ | 16.0 mm | 16.3 mm | 0.8 |
| $a_2$ | 32.0 mm | 33.3 mm | 4.2 |
| $a_3$ | 16.0 mm | 16.3 mm | 1.7 |
| $d_{12}$ | 4.86 mm | 5.25 mm | 8.0 |
| $d_{23}$ | 4.86 mm | 5.25 mm | 8.0 |
| $h$ | 238.2 mm | 224.4 mm | –5.8 |
| $N$ | 14 | 14 | 0 |

TABLE V
ESTIMATED WINDING PARAMETERS OF A UTILITY 167 kVA, 14.4 kV/120–240 V, SINGLE-PHASE TRANSFORMER

| Parameter | Actual | Estimated | Error (%) |
|---|---|---|---|
| $r_1$ | 123.6 mm | 129.8 mm | 4.9 |
| $r_2$ | 162.4 mm | 167.4 mm | 3.1 |
| $r_3$ | 201.2 mm | 205.0 mm | 1.9 |
| $a_1$ | 16.0 mm | 16.7 mm | 4.5 |
| $a_2$ | 43.7 mm | 40.9 mm | –6.5 |
| $a_3$ | 16.0 mm | 16.7 mm | 4.5 |
| $d_{12}$ | 8.89 mm | 8.82 mm | –0.8 |
| $d_{23}$ | 8.89 mm | 8.82 mm | –0.8 |
| $h$ | 263.5 mm | 280.0 mm | 6.3 |
| $N$ | 9 | 9 | 0 |

winding. This introduces undesirable errors in the calculations. In addition, for our small transformers, insulation distances and winding thicknesses are very small. Therefore, the errors associated with their measurement (using a Vernier) are not negligible in relative terms. For instance, take the 1.8 kVA transformer presented in Table II, the difference between the estimated and measured value for the thickness of winding 3 is less than 0.5 mm but it shows as a relative error of 12%. Thus, the winding thickness can be determined with very small absolute error (under half a millimeter), that became a relatively large error (12%). These relatively large errors are negligible on the overall design and performance of the transformer. It can be seen from the calculations made on the 75 and 167 kVA transformers that the estimated and actual values match more closely.

## IV. CALCULATION OF THE GEOMETRICAL INFORMATION OF THE IRON CORE

The knowledge of the cross sectional area and the physical or relative dimensions of the iron core are imperative when building a transformer model capable of accurately representing the iron core behavior in low- and high-frequency transients [9], [28]–[30].

In this section multiple expressions have been derived to approximate the core design characteristics such as cross sectional area and length of limbs and yokes. These equations are based on the simple geometrical rules that utilize the winding parameters obtained in the previous section.

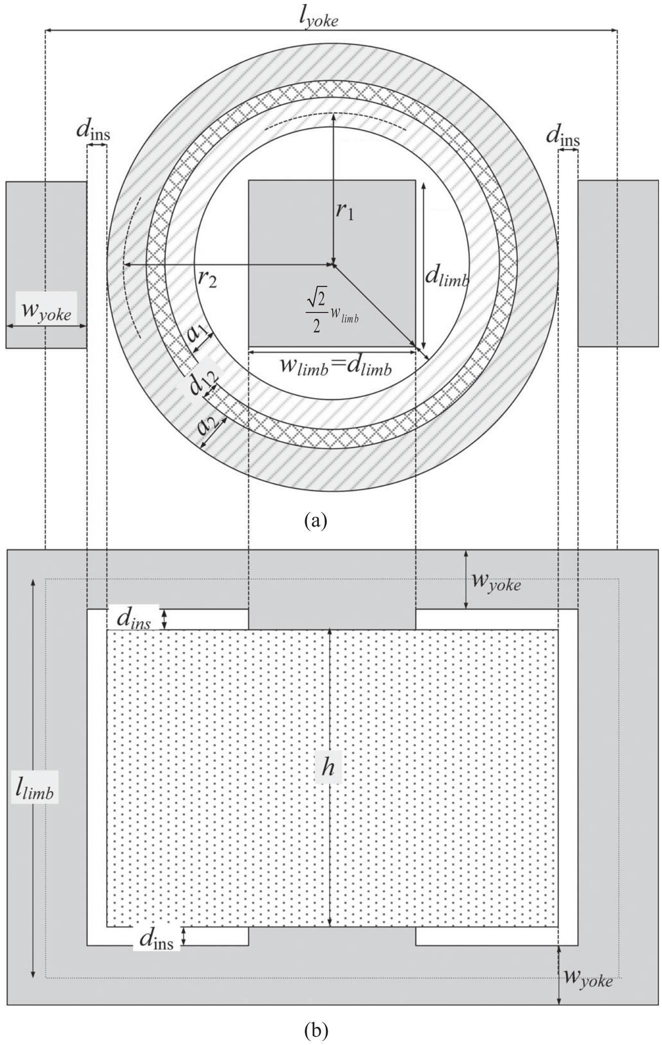


Fig. 6. Transformer core and windings; (a) top view; (b) side view.

Note that in all the calculations for small transformers, winding thicknesses and insulation distances have been neglected for simplicity. Furthermore, neglecting these parameters compensates for the effects of the simplifying assumptions made on the geometry of the core cross-section (such as assuming a square core cross section versus rectangular cross-section).

As illustrated in Fig. 6(a), the limb of the core is encircled by the inner-most winding. Hence, the diameter of the limb equals the inner diameter of the low voltage winding neglecting the insulation distance. Considering the assumptions made for the dimensions of the core, after the application of simple geometrical rules, the cross sectional area for the limb can be computed from:

$$A = d_{limb} \times w_{limb} = \left[\sqrt{2}(r_1)\right]^2 = 2{r_1}^2 \tag{15}$$

Remember from Section II that $r_1$ represents the mean radius of the low voltage (inner-most) winding, $r_2$ is mean radius of the high voltage (outer-most) winding, $d_{limb}$ and $w_{limb}$ denote the depth and width of the limb, $d_{yoke}$ and $w_{yoke}$ denote the depth and width of the yoke respectively. The cross sectional area of the yoke $A_{yoke}$ is assumed to be half of the limb cross sectional area as discussed previously.

TABLE VI
ESTIMATED DIMENSIONS OF A 4-WINDING 1 KVA, 120–240/120–240 V, SINGLE-PHASE TRANSFORMER CORE

| Parameter | Actual | Estimated | Error (%) |
|---|---|---|---|
| $l_{yoke}$ | 115 mm | 106.2 mm | –7.6 |
| $A_{yoke}$ | 15.1 cm$^2$ | 16.5 cm$^2$ | 9.2 |
| $l_{limb}$ | 85 mm | 87.2 mm | 2.6 |
| $A_{limb}$ | 34.5 cm$^2$ | 33.1 cm$^2$ | –4.0 |

We believe that the method can be extended to larger transformers, which are built with staked laminations of different widths. The core cross section can be considered cylindrical similar to the windings which makes the calculations less complicated. In this case, the core radius can be obtained from:

$$r_{limb} = r_1 - \frac{a_1}{2} - d_{12} \tag{16}$$

where $r_{limb}$ denotes the limb radius. The limb and yoke cross sectional areas are calculated accordingly. However, full validation remains to be done against practical data.

The lengths of the yoke and limb ($l_{yoke}$ and $l_{limb}$) can also be estimated using the windings dimensions. $l_{yoke}$ is calculated by adding the diameter of the outermost winding to the width of the yoke, neglecting the insulation distances as mentioned earlier, ($l_{yoke} = 2r_2 + w_{yoke}$); see Fig. 6. $l_{limb}$ is computed as the height of the winding plus the width of the yoke ($l_{limb} = h + w_{yoke}$); see Fig. 6(b).

The shape of the bobbins for distribution transformers is more frequently rectangular than cylindrical. Therefore, the cylindrical assumptions might not be very accurate in these cases for geometrical calculations since considering the same perimeter, the calculated radius (if cylindrical), becomes larger than the actual width and smaller than the actual length (if rectangular). Calculation results show that, these equations can overestimate the length of the yoke. Hence, to overcome this challenge, the winding thicknesses and insulating distances have been neglected in the calculations. In addition, the solution of equations is bounded by the external dimensions of transformer tank (length of the transformer tank minus width of the yoke). As a result, $l_{yoke}$ can be estimated by taking the minimum of the value calculated using the dimensions of the windings and the upper bound enforced by the external dimensions of the transformer. Consequently, length of the yoke is approximated by:

$$\begin{aligned} l_{yoke} &= \min\left[(2r_2 + w_{yoke}), (l_{tank} - w_{yoke})\right] \\ &= \min\left[\left(2r_2 + \frac{r_1}{\sqrt{2}}\right), \left(l_{tank} - \frac{r_1}{\sqrt{2}}\right)\right] \end{aligned} \tag{17}$$

The length of the limb ($l_{limb}$) is approximated by taking the minimum of the values calculated using the average height of the windings and the upper band enforced by the external dimensions of the transformer tank (height of the tank minus width of

TABLE VII
ESTIMATED DIMENSIONS OF A 4-WINDING 1.8 KVA, 120–240/120–240 V, SINGLE-PHASE TRANSFORMER CORE

| Parameter | Actual | Estimated | Error (%) |
|---|---|---|---|
| $l_{yoke}$ | 126.3 mm | 130.8 mm | 3.6 |
| $A_{yoke}$ | 23.4 cm$^2$ | 21.8 cm$^2$ | –6.8 |
| $l_{limb}$ | 101.3 mm | 104.4 mm | 3.1 |
| $A_{limb}$ | 44.8 cm$^2$ | 43.5 cm$^2$ | –2.9 |

TABLE VIII
ESTIMATED DIMENSIONS OF A 4-WINDING 5 KVA, 120–240/480–960 V, SINGLE-PHASE TRANSFORMER CORE

| Parameter | Actual | Estimated | Error (%) |
|---|---|---|---|
| $l_{yoke}$ | 190.5 mm | 206.2 mm | 8.2 |
| $A_{yoke}$ | 52.0 cm$^2$ | 47.5 cm$^2$ | –8.6 |
| $l_{limb}$ | 151.1 mm | 137.4 mm | –9.0 |
| $A_{limb}$ | 104.0 cm$^2$ | 95.0 cm$^2$ | –8.6 |

TABLE IX
ESTIMATED DIMENSIONS OF A UTILITY 75 KVA, 7.2 KV/120–240 V, SINGLE-PHASE TRANSFORMER CORE

| Parameter | Actual | Estimated | Error (%) |
|---|---|---|---|
| $l_{yoke}$ | 328.3 mm | 347.4 mm | 7.3 |
| $A_{yoke}$ | 111.7 cm$^2$ | 105.4 cm$^2$ | –5.6 |
| $l_{limb}$ | 306.3 mm | 297.0 mm | –3.0 |
| $A_{limb}$ | 223.5 cm$^2$ | 210.8 cm$^2$ | –5.7 |

the yoke):

$$l_{limb} = \min\left[(h + w_{yoke}), (h_{tank} - w_{yoke})\right] = \min\left[\left(h + \frac{r_1}{\sqrt{2}}\right), \left(h_{tank} - \frac{r_1}{\sqrt{2}}\right)\right] \quad (18)$$

where $h_{tank}$ and $l_{tank}$ are height and length of the transformer tank, respectively. In case of large transformers, the $w_{yoke}$ can be replaced by $r_{limb}$ in (16).

The results for the core dimensions of the 4-winding 1 kVA, 120–240/120–240 V transformer described in the previous section are given in Table VI. The accuracy is high for most of the parameters and around 9% in the worst case. Similarly the estimation results for the 4-winding, 1.8 kVA, 120–240/120–240 V, single-phase transformer is presented in Table VII. The results are accurate for all parameters with less than 7% relative error. The results for 5 kVA, 120–240/480–960 V transformer are presented in Table VIII showing acceptable accuracy as in the previous cases with maximum relative error of around 9%. Table IX contains the calculation results for the core dimensions of the 75 kVA, 7.2 kV-120/240 V transformer. The obtained results show an acceptable engineering accuracy, with the largest error of around 7%. The results for the 167 kVA, 14.4 kV/120–240 V transformer are presented in Table X. The calculated dimensions show good accuracy with largest error of 5%.

TABLE X
ESTIMATED DIMENSIONS OF A UTILITY 167 KVA, 14.4 KV/120–240 V, SINGLE-PHASE TRANSFORMER CORE

| Parameter | Actual | Estimated | Error (%) |
|---|---|---|---|
| $l_{yoke}$ | 410.5 mm | 428.2 mm | 4.3 |
| $A_{yoke}$ | 162.6 cm$^2$ | 163.4 cm$^2$ | 0.5 |
| $l_{limb}$ | 346.1 mm | 358.2 mm | 3.5 |
| $A_{limb}$ | 325.2 cm$^2$ | 333.8 cm$^2$ | –5.2 |

## V. CONCLUSION

In this paper a non-destructive method has been proposed to estimate the design parameters of single-phase distribution transformers using electrical terminal measurements and nameplate data. Transformer characteristics such as leakage and saturation inductances along with winding dc resistances have been measured using standard or proposed tests. The dependence of the measured characteristics on the internal dimensions of the transformer has been utilized to estimate the winding dimensions and the number of turns in each winding with acceptable engineering accuracy.

The dimensions of the core and cross sectional areas of the limb and the yokes have been estimated using the results from the solution of a system of equations bounded by external dimensions of the transformer tank. Overall, the computational results are accurate, despite of the diversity of the calculated parameters.

The proposed method is capable of calculating the radii, thickness, and height of all windings. It can also compute the inter-winding insulating spaces which are not possible with the estimation methods based on external dimensions of the transformer. In addition, this method is applicable to a wide range of single-phase distribution transformers since it uses electrical measurements linked directly to design equations.

## ACKNOWLEDGMENT

The authors would like to thank Dr. Juan Carlos Olivares from Universidad Autónoma Metropolitana (Azcapotzalco), México, for information and useful discussions on transformer design. The last author would like to thank Mr. Val Tatu from Pioneer Transformers for years of valuable discussions on transformer design and construction.

## REFERENCES

[1] F. Gonzalez-Molina, D. Ishchenko, and B. A. Mork, “Parameter estimation and advancements in transformer models for EMTP simulations,” Task/Activity MTU-6: Parameter Estimation, Bonneville Power Administration, Dec. 2003.
[2] W. G. Enright, O. B. Nayak, G. D. Irwin, and J. Arrillaga, “An electromagnetic transients model of multi-limb transformer using normalized core concept,” in *Proc. Int. Conf. Power Syst. Transients*, Seattle, WA, USA, Jun. 1997, pp. 93–98.
[3] S. Jazebi, F. de León, A. Farazmand, and D. Deswal, “Dual reversible transformer model for the calculation of low-frequency transients,” *IEEE Trans. Power Del.*, vol. 28, no. 4, pp. 2509–2517, Oct. 2013.
[4] J. Faiz, B. M. Ebrahimi, and T. Noori, “Three- and two-dimensional finite-element computation of inrush current and short-circuit electromagnetic forces on windings of a three-phase core-type power transformer,” *IEEE Trans. Magn.*, vol. 44, no. 5, pp. 590–597, May 2008.

[5] A. Shintemirov, W. Tang, and Q. Wu, "A hybrid winding model of disc-type power transformers for frequency response analysis," *IEEE Trans. Power Del.*, vol. 24, no. 2, pp. 730–739, Apr. 2009.

[6] P. Mukherjee and L. Satish, "Construction of equivalent circuit of a single and isolated transformer winding from FRA data using the ABC algorithm," *IEEE Trans. Power Del.*, vol. 27, no. 2, pp. 963–970, Apr. 2012.

[7] A. Rezaei-Zare, "Enhanced transformer model for low- and mid-frequency transients—Part I: Model development," *IEEE Trans. Power Del.*, vol. 30, no. 1, pp. 307–315, Feb. 2015.

[8] S. D. Mitchell and J. S. Welsh, "Initial parameter estimates and constraints to support gray box modeling of power transformers," *IEEE Trans. Power Del.*, vol. 28, no. 4, pp. 2411–2418, Oct. 2013.

[9] S. D. Cho, "Parameter estimation for transformer modeling," Ph.D. dissertation, Dept. Elect. Comput. Eng., Michigan Tech. Univ., Houghton, MI, USA, 2002.

[10] B. Gustavsen and A. Portillo, "Interfacing k-factor based white-box transformer models with electromagnetic transients programs," *IEEE Trans. Power Del.*, vol. 29, no. 6, pp. 2534–2542, Dec. 2014.

[11] K. Ragavan and L. Satish, "Construction of physically realizable driving-point function from measured frequency response data on a model winding," *IEEE Trans. Power Del.*, vol. 23, no. 2, pp. 760–767, Apr. 2008.

[12] S. Mitchell and J. Welsh, "Modeling power transformers to support the interpretation of frequency-response analysis," *IEEE Trans. Power Del.*, vol. 26, no. 4, pp. 2705–2717, Oct. 2011.

[13] Z. W. Zhang, W. H. Tang, Q. H. Wu, and J. D. Yan, "Detection of minor axial winding movement within power transformers using finite element modeling," in *Proc. IEEE PES Gen. Meeting Conf. Expo.*, 2014, pp. 1–5.

[14] E. Rahimpour, J. Christian, K. Feser, and H. Mohseni, "Transfer function method to diagnose axial displacement and radial deformation of transformer windings," *IEEE Trans. Power Del.*, vol. 18, no. 2, pp. 493–505, Apr. 2003.

[15] J. Sandraz, F. de León, and J. Cultrera, "Validated transient heat transfer model of underground transformer in rectangular vaults," *IEEE Trans. Power Del.*, vol. 28, no. 3, pp. 1770–1778, Jul. 2013.

[16] *Standard for the Design, Testing, and Application of Liquid-Immersed Distribution, Power, and Regulating Transformers Using High-Temperature Insulation Systems and Operating at Elevated Temperatures*, IEEE Std. C57.104-2012, 2012.

[17] F. de León and J. A. Martinez, "Dual three-winding transformer equivalent circuit matching leakage measurements," *IEEE Trans. Power Del.*, vol. 24, no. 1, pp. 160–168, Jan. 2009.

[18] S. V. Kulkarni and S. A. Khaparde, *Transformer Engineering: Design and Practice*. New York, NY, USA: Marcel Dekker, May 2004.

[19] M. Lambert, F. Sirois, M. Martínez-Duró, and J. Mahseredjian, "Analytical calculation of leakage inductance for low-frequency transformer modeling," *IEEE Trans. Power Del.*, vol. 28, no. 1, pp. 507–515, Jan. 2013.

[20] F. de León, S. Jazebi, and A. Farazmand, "Accurate measurement of the air-core inductance of iron-core transformers with a non-ideal low power rectifier," *IEEE Trans. Power Del.*, vol. 29, no. 1, pp. 294–296, Feb. 2014.

[21] F. de León, A. Farazmand, S. Jazebi, D. Deswal, and R. Revi, "Elimination of residual flux in transformers by the application of an alternating polarity dc voltage source," *IEEE Trans. Power Del.*, vol. 30, no. 4, pp. 1727–1734, Aug. 2015.

[22] E. P. Dick and W. Watson, "Transformer models for transient studies based on field measurements," *IEEE Trans Power Appl. Syst.*, vol. PAS-100, no. 1, pp. 409–418, Jan. 1981.

[23] C. G. A. Koreman, "Determination of the magnetizing characteristic of three-phase transformers in field tests," *IEEE Trans. Power Del.*, vol. 4, no. 3, pp. 1779–1785, Jul. 1989.

[24] S. Abdulsalam, W. Xu, W. L. A. Neves, and X. Liu, "Estimation of transformer saturation characteristics from inrush current waveforms," *IEEE Trans. Power Del.*, vol. 21, no. 1, pp. 170–177, Jan. 2006.

[25] L. Cohen, "An exact formula for the mutual inductance of coaxial solenoids," *Bull. Bureau Standards*, vol. 3, no. 2, pp. 295–303, May 1907.

[26] T. H. Fawzi and P. Burke, "The accurate computation of self and mutual inductance of circular coils," *IEEE Trans. Power App. Syst.*, vol. PAS-97, no. 2, pp. 464–468, Apr. 1978.

[27] I. Dasgupta, *Design of Transformers*. Delhi, India: Tata McGraw-Hill Edu., 2002.

[28] S. E. Zirka, Y. I. Moroz, C. M. Arturi, N. Chiesa, and H. K. Høidalen, "Topology-correct reversible transformer model," *IEEE Trans. Power Del.*, vol. 27, no. 4, pp. 2037–2045, Oct. 2012.

[29] A. Shintemirov, W. Tang, and Q. Wu, "Transformer core parameter identification using frequency response analysis," *IEEE Trans. Magn.*, vol. 46, no. 1, pp. 141–149, Jan. 2010.

[30] B. A. Mork, F. Gonzalez, D. Ishchenko, D. L. Stuehm, and J. Mitra, "Hybrid transformer model for transient simulation—Part I: Development and parameters," *IEEE Trans. Power Del.*, vol. 22, no. 1, pp. 248–255, Jan. 2007.

[31] C. W. T. McLyman, *Transformer and Inductor Design Handbook*. New York, NY, USA: Marcel Dekker, 2016.


**Reza Kazemi** (S'08) received the B.Sc. and M.Sc. degrees in electrical engineering with a focus on power and energy from Amirkabir University of Technology (Tehran Polytechnic), Tehran, Iran, in 2009 and 2012, respectively. Since 2014, he has been working toward the Ph.D. degree in the Department of Electrical and Computer Engineering, New York University.

His research interests include electromagnetic modeling of electrical power components, transient and steady-state analysis of power systems, integration of renewable energy sources to power networks and power market studies.

**Saeed Jazebi** (S'10–M'14–SM'16) received the B.Sc. degree from Shahid Bahonar University, Kerman, Iran, in 2006, the M.Sc. degree from Amirkabir University of Technology, Tehran, Iran, in 2008, and the Ph.D. degree from New York University, Brooklyn, NY, USA, in 2014, all in electrical engineering.

He is continuing his research as a Postdoctoral Fellow at New York University. His fields of interest include electromagnetic design, modeling, and simulation of electrical machines and power system components, power system protection, and power quality.

**Digvijay Deswal** (S'16) received the B.Tech. and M.Tech. degrees in electrical engineering from the Indian Institute of Technology Kharagpur, West Bengal, India, in 2014. He is currently working toward the Ph.D. degree at New York University School of Engineering.

His research interests include machine design, power electronics, and analysis of electrical machines.

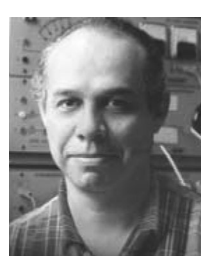

**Francisco de León** (S'86–M'92–SM'02–F'15) received the B.Sc. and M.Sc. (Hons.) degrees from the National Polytechnic Institute, Mexico City, Mexico, in 1983 and 1986, respectively, and the Ph.D. degree from the University of Toronto, Toronto, ON, Canada, in 1992, all in electrical engineering.

He has held several academic positions in Mexico and has worked for the Canadian electric industry. He is currently an Associate Professor in the Department of Electrical and Computer Engineering, New York University. His research interests include the analysis of power phenomena under nonsinusoidal conditions, the transient and steady-state analyses of power systems, the thermal rating of cables and transformers, and the calculation of electromagnetic fields applied to machine design and modeling.

Dr. de León is an Editor of IEEE TRANSACTIONS ON POWER DELIVERY and IEEE POWER ENGINEERING LETTERS.